Journal of Solid State Chemistry 184 (2011) 2285–2292

Contents lists available at ScienceDirect

Journal of Solid State Chemistry

journal homepage: www.elsevier.com/locate/jssc

Selective formation of VO_2(A) or VO_2(R) polymorph by controlling the hydrothermal pressure

Shidong Ji [a,b], Feng Zhang [b], Ping Jin [c,*]

[a] College of Materials Science and Technology, Nanjing University of Technology, No. 5, New Mofan Road, 210009 Nanjing, China
[b] Department of Scientific and Engineering Simulation, Nagoya Institute of Technology, Gokiso-Cho, Showa-ku, Nagoya 466-8555, Japan
[c] Research Center for Industrial Ceramics, Shanghai Institute of Ceramics, Chinese Academy of Sciences, Dingxi Road 1295, Changning, Shanghai 200050, China

ARTICLE INFO

Article history:
Received 3 March 2011
Received in revised form
17 June 2011
Accepted 24 June 2011
Available online 1 July 2011

Keywords:
Hydrothermal treatment
VO_2 polymorphs
Phase transformation
Ground state energy
Pressure

ABSTRACT

Missing VO_2(A) usually occurs during the preparation of VO_2 polymorphs. This leads to an ambiguous understanding of the transformation between VO_2 polymorphs. The calculation of the ground state energies for different VO_2 polymorphs indicated that there is only a small energy gap between VO_2(A) and VO_2(R), which destined that the transformation from VO_2(A) to VO_2(R) should be pressure sensitive. This hypothesis was verified during the synthesizing of VO_2 polymorphs by reducing V_2O_5 with oxalic acid through hydrothermal treatment process. Selective formation of pure phase VO_2(A) or VO_2(R) was achieved by controlling the hydrothermal pressure through varying the filling ratio at 270 °C. It was found that a filling ratio over 0.5 favors the formation of pure VO_2(R) while a reduced filling ratio to 0.4 or lower results in the formation of VO_2(A). Based on our experiments, VO_2(B) nanobelts were always first formed and then it transformed to VO_2(A) by assembling process at increased temperature or extended reaction time. Under further higher pressure, the VO_2(A) transformed spontaneously to VO_2(R) initialized from the volume shrinkage due to the formation of denser VO_2(R).

1. Introduction

Vanadium dioxide (VO_2) is a typical binary compound with different polymorphs. The polymorphic varieties in this system include tetragonal rutile-type VO_2(R) [1] monoclinic VO_2(M) [2] and at least three metastable phases named as VO_2(B), VO_2(A) [3,4] and VO_2(C) [5]. The diversity of this material endows it as a good study object in theoretical and experimental condensed matter and a broad application in many fields [6]. As a transition metal oxide with narrow *d*-electron bands and strongly correlated electron effect, the stable rutile-type VO_2(R) phase has attracted much interest because of the reversible phase transition at about 340 K [7]. Accompanied with this first-order phase transition, VO_2(R) shows a reversible abrupt change of electric and magnetic properties and a sharp variation of optical transmittance especially in IR region [8,9]. These properties make it candidates for many promising applications in diverse fields, such as gas and temperature sensors [10], optical switching devices [11], optical date storage medium [12] and smart windows [13]. Other metastable polymorphs, especially for VO_2(B), also have been researched for a long time. Owing to its low cost, relatively low toxicity, abundant in nature, high energy capacity and moderate work-potential, metastable VO_2(B) has been considered to be the potential candidate for cathode in lithium cells for electric vehicles (EVs) or hybrid EVs (HEVs) [14]. Through preparing nano-textured VO_2(B) cathode from vanadium oxide aerogels, amazing specific capacity as high as 500 mAh/g was reported by Baudrin group [15]. High capacity and high capacity maintaining properties were also shown by Zhou's group [16] through designing and synthesizing a novel nanothorn VO_2(B) hollow microsphere. All these studies revealed that the layer structure VO_2(B) had high Li^+ intercalation performance. However, another layer structure metastable polymorph—VO_2(A) had not been studied widely until now. One main reason is that this metastable phase is usually missed during the preparation of VO_2 polymorphs. VO_2(A) was first reported by Theobald [4] as a new metastable phase, which bridges the transformation from metastable VO_2(B) to stable VO_2(R) in the extensive study of hydrothermal synthesis of vanadium oxides and oxyhydroxides in V_2O_4–V_2O_5–H_2O system. A couple of decades later, Oka et al. measured the crystal structures of low-temperature and high-temperature VO_2(A) phase [17,18]. There have been few works on VO_2(A) reported thereafter.

Along with the recognizing of the importance about VO_2 material, various strategies have been developed for the preparation of VO_2 or VO_2-related devices. Thin films of thermochromic VO_2(R) have been deposited by magnetron sputtering, ion-beam sputtering, electron beam evaporation, chemical vapor deposition, sol–gel, reactive decomposition, evaporative decomposition of solution, etc. [19]. In some of these processes, polycrystalline VO_2(R) film was fabricated by annealing amorphous or metastable VO_2(B) film [20]. Meanwhile, VO_2 powder with different

* Corresponding author.
E-mail address: p-Jin@mail.sic.ac.cn (P. Jin).

0022-4596/$ - see front matter © 2011 Elsevier Inc. All rights reserved.
doi:10.1016/j.jssc.2011.06.029

polymorphs and nanostructures has been prepared using a number of techniques. These mainly include the reducing of KVO_3 with KBH_4 [21], pyrolyzing the vanadium containing precursor [22], sol–gel method and hydrothermal synthesis method [23–25]. However, it should be noticed that most of these works focused on the preparation of VO_2(R) or VO_2(B) single phase and successful fabrication of VO_2(A) was seldom reported until now. Furthermore, the transition relationship between metastable phases and stable VO_2(R/M) phase has not been revealed sufficiently. It could be found easily from the literature that the absence of VO_2(A) during the preparation and/or the transition processes puzzled many scientists. For example, Leroux et al. [26] reported their results about the research of the intermediate steps of the phase transition between the metastable monoclinic VO_2(B) phase and the stable tetragonal rutile VO_2(R) phase by in situ electron microscopy. They clearly declared that no evidence for the presence of VO_2(A) at any stage during the transformation was present. Gui et al. [27] prepared VO_2(R) nanorods by annealing VO_2 hydrate at various temperatures ranging from 200 to 500 °C and no metastable VO_2 phase was detected during this process.

Selective formation of VO_2 polymorphs is still a challenge for material scientists. Thermodynamically, the existence of one special morph of VO_2 depends on thermodynamic conditions, which mainly include system pressure (p), temperature (T) and chemical circumstance. Based on the general consensus that the chemical valency of vanadium is mainly controlled by chemical circumstance, the relationship between other thermodynamic parameters, especially for temperature, and phase transition between VO_2 polymorphs has been studied widely. For instance, to obtain thermochromic VO_2(R) powder, many researchers took the annealing of metastable VO_2(B) [28] phase or VO_2 hydrates [29] as an effective approach. However, the importance of another thermodynamic parameter, p, has not aroused enough attention. Without the consideration of this important thermodynamic parameter, it is impossible to establish correct and complete image about the relationship between VO_2 polymorphs.

Recently, the effect of tungsten doping on VO_2(A) was studied by our group [30]. It was found that slightly over-doping of tungsten would lead VO_2(A) destable and it excited our interest in the study to reveal the intrinsic properties of this metastable phase. To avoid the influence of other cations, a simple V_2O_5–$H_2C_2O_4$–H_2O system was still adopted in this paper and it was found that the system pressure was a key parameter for the control of the final phase. The fabrication of VO_2(B), VO_2(A) and/or VO_2(R) and their transition could be controlled in this system by varying the system pressure during hydrothermal treatment. Based on the calculation of ground state energies for VO_2 polymorphs, the thermodynamic relationship between these three phases and the special metastable properties of VO_2(A) phase were successfully disclosed.

2. Experimental

2.1. Synthesis

The VO_2 powders were synthesized by hydrothermal method using V_2O_5 (Wako, Japan) as the source of vanadium and oxalic acid ($H_2C_2O_4 \cdot 2H_2O$, Wako, Japan) as a reducing agent. All of the chemical reagents in our experiments were of analytical grade and used without further purification. In a typical procedure, the appropriate amount of V_2O_5 and oxalic acid (1:(1–3) in molar ratio) solid powders was directly added to 200 ml deionized water followed by pre-reduction at room temperature. The suspension was continuously stirred until a clear dark blue transparent solution was formed. In this paper, hydrothermal treatments for this solution were carried out mainly at 270 °C with different filling ratios (designated as f in the captions of the following figures) in Teflon-lined autoclave (25 ml in capacity) with a stainless steel shell holding for different periods of time under auto-generated pressure.

After hydrothermal treatment, the autoclave was cooled naturally to room temperature. The resulting precipitates were collected by filtering, washed with acetone and dehydrated alcohol several times and then dried in air at 60 °C for 10 h.

2.2. Characterization

X-ray powder diffraction (XRD) analysis was conducted on a Philips X'Pert diffractometer at a scanning rate of 2° per minute with 2θ ranging from 10° to 70°, using graphite monochromated Cu$K\alpha$1 radiation ($\lambda = 0.154056$ nm) at 30 KV accelerating voltage and 40 mA current. The morphologies of the prepared particles were observed by field emission scanning electrical microscopy (FE-SEM, HITACHI S-3400, Japan) at an acceleration voltage of 10 KV and transmission electron microscopy (TEM, JEOL JEM-2010, Japan) operated at 200 KV. The attachment of selected area electron diffraction (SAED) of JEM-2010 was used to get the crystallographic information. X-ray photoelectron spectra (XPS) were collected on X-ray photoelectron spectrometer (Σprobe, Thermo VG Scientific, United Kingdom) with an exciting source of Mg$K\alpha$ (1253.6 eV). Phase transition temperature and its hysteresis property were measured by differential scanning calorimetry (DSC120, SEIKO, Japan) in a heating or cooling rate at 2 °C/min with a liquid nitrogen cooling unit.

2.3. Computational

The ground state energies of VO_2(A)(HT) (high-temperature VO_2(A) phase) [18], VO_2(B) and VO_2(R) phases were calculated using the standard Cambridge Sequential Total Energy Package (CASTEP) code, which is a plane-wave pseudo-potential total energy calculation method based on density function theory (DFT) from the first principles (*ab initio*) [31]. Before energy calculation, the lattice parameters were optimized. The plane-wave energy cut-off and the Brillouin zone sampling were fixed at 450 eV and $6 \times 6 \times 4$ special k-point meshes, respectively. Interactions of electrons with ion cores were represented by the Vanderbilt-type ultrasoft pseudo-potential. The electronic exchange-correction energy was treated according to the local density approximation (LDA) [32] with Ceperley–Alder and Perdew–Zunger (CA–PZ) [33,34] exchange-correction potential. The crystal structures were fully optimized by independently modifying lattice parameters and internal atom coordinates. The Broyden–Fletcher–Goldfarb–Shanno (BFGS) [35] minimization scheme was used to minimize the total energy and internal forces. The tolerances for geometry optimization were set as the difference in total energy being within 5×10^{-6} eV/atom, the maximum ionic Hellmann–Feynman force being within 5×10^{-5} nm and the maximum stress being within 0.02 GPa.

3. Results and discussion

3.1. Pressure and filling ratio

It is well known that there is a close relationship between filling ratio and auto-generated pressure in hydrothermal treatment process [36]. For water, there is a critical filling ratio, which depends on temperature in hydrothermal treatment. Extreme high pressure would be caused by the expansion of liquid water

when the filling ratio is higher than the critical filling ratio and in the absence of vapor phase. When the filling ratio is lower than the critical one, the liquid water phase and vapor water phase should coexist in the autoclave. In this case, the saturated pressure in the autoclave depends only on the temperature. These data can be calculated from some approximate equations or obtained from some database, such as "International Saturated Steam Table". Here we take the equilibrium pressure of 5.503 MPa from that table as reference. The practical pressure was measured by heating a portable reactor (TVS-N2, Taiatsu, Japan) at 270 °C using deionized water and real reaction solution separately with different filling ratios. These data are listed in Table 1.

For water, the measured values are close to the reference and there is no significant difference between these values for different filling ratios (f=0.4–0.6). These results showed that the filling ratio of 0.60 did not surpass the critical filling ratio for water at 270 °C. However, the real reaction system in our experiments is divergent from pure water. The main reaction during hydrothermal treatment for the formation of VO_2 could be formulated as the following:

$$V_2O_5 + H_2C_2O_4 = 2VO_2 + H_2O + 2CO_2\uparrow$$

The chemical reagents and their reaction made this system complex and the auto-generated pressure during hydrothermal treatment seemed unsolvable through calculation. The elevation of pressure for real system would be considered as the contribution of CO_2 produced following the previous reaction. The solubility of CO_2 mainly depends on temperature and pressure. With the increase in filling ratio, the generated amount of CO_2 increases and the volume accommodating the vapor phase decreases. So the elevation of pressure could be observed when the filling ratio increases.

3.2. Influence of temperature and filling ratio on the resulted phases

The XPS spectra of a typical sample are shown in Fig. 1. No peaks of elements other than C, O and V could be observed on the survey spectrum (Fig. 1(a)). The peaks for C could be attributed to the CO_2 adsorbed on the surfaces of the sample or the contaminant from the conductive carbon tape used to bind the powders. The V_{2p} binding energies with the center at 516.10 eV for $V_{2p3/2}$ and 523.40 eV for $V_{2p1/2}$ (Fig. 1(b)) and the intensity ratio, which is near 2:1 [37], between these two peaks are characteristic values of vanadium in +4 oxidation state, which are well consistent with the values of bulk VO_2 reported in the literature [38].

Table 1
Pressure in autoclave after heating water and real reaction solution at 270 °C for 24 h.

Item	f=0.4	f=0.5	f=0.6
Pressure for water (MPa)	5.31	5.30	5.30
Pressure for real solution (MPa)	6.45	7.30	9.28

It was interesting to note that while the XPS spectra were almost the same for different samples of VO_2(B), VO_2(A) and VO_2(R) or the mixture of them, the appearances of these polymorphs were obviously different. For example, VO_2(A) phase was reddish-brown fluffy fibrous powder with nice dispersity, while fine VO_2(B) powder was gray black and the density paper-like cake could be formed preferably after filtering and the color of VO_2(R) powder was relatively black without obvious aggregation.

Fig. 2 shows the XRD patterns for samples synthesized at different temperatures holding for 24 h under the filling ratio of 0.40. All the peaks of these samples could be indexed thoroughly to PDF files of 01-075-6403 for VO_2(A) and/or 01-081-2392 for VO_2(B) and no peaks belonging to VO_2(R) could be found in these XRD patterns. Pure VO_2(A) could be obtained when the hydrothermal treatment temperature was higher than 230 °C, while lower temperature was beneficial for the formation of VO_2(B) phase. In our experiments, pure VO_2(B) could be obtained by hydrothermal treatment at 180 °C. Transformation from VO_2(B) to VO_2(A) could occur during the temperature range from 180 to 230 °C.

Besides temperature, system pressure was found to be a very important factor, which has a great influence on the formation of

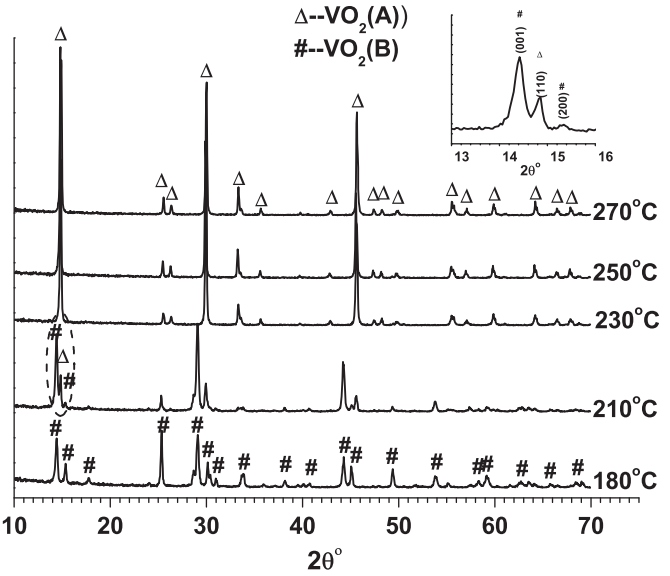

Fig. 2. XRD patterns for samples synthesized at different temperatures for 24 h with the filling ratio of 0.40 (f=0.40) (inset was the enlarged pattern of the circled part showing the mixture of VO_2(B) and VO_2(A)).

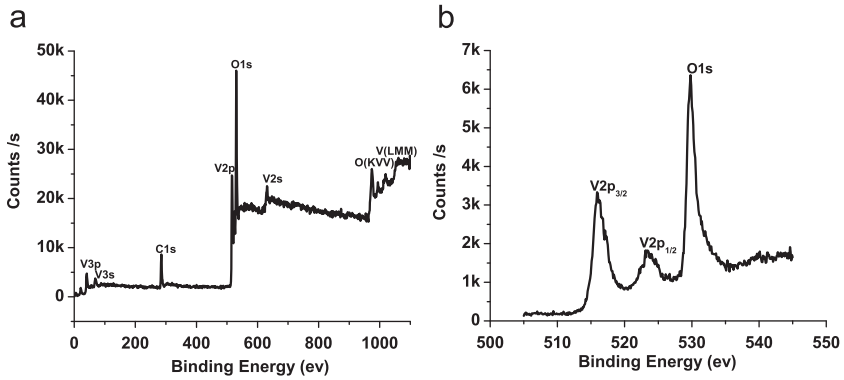

Fig. 1. XPS spectra of typical VO_2 powder as-prepared: (a) survey spectrum; (b) core-level spectrum of V_{2p} and O_{1s}.

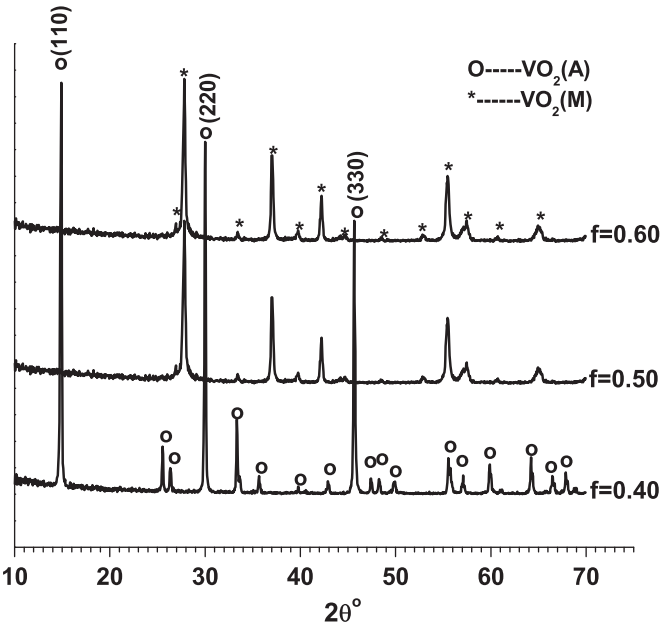

Fig. 3. XRD patterns for samples prepared at 270 °C for 24 h with the filling ratios (f) varied from 0.40 to 0.60.

the final VO_2 polymorphs. In this work, the system pressure was controlled by varying the filling ratio and the corresponding XRD patterns are shown in Fig. 3. It has been revealed that the auto-generated pressure in hermetic vessel during hydrothermal treatment process was dependent on filling ratio when temperature and the chemical constitution were kept unchanged in our reaction system. The auto-generated pressure (p) became high with the increase in filling ratio or the increase in temperature. When the filling ratio increased from 0.40 to 0.50 or 0.60, VO_2(A) phase thoroughly transformed to VO_2(R/M) phase after 24 h of hydrothermal treatment at 270 °C. Comparison experiments were also conducted at 250 °C for 24 h. In this condition, only a small part of VO_2(A) transformed to VO_2(R) under the filling ratio of 0.60 and VO_2(A) was almost kept unchanged under the filling ratio of 0.50. Solely extending the holding time could not bring about this dramatic change when the system pressure was lower, which corresponds to the state of lower filling ratio during hydrothermal treatment in our experiments. For instance, while the particles of VO_2(A) rods grew evidently, this phase seems intact after holding the autoclave at 270 °C for 7 days with the filling ratio of 0.40 or less.

3.3. Thermodynamic analysis for the pressure related phase transformation

The phenomenon of pressure dependent VO_2 polymorphs could be qualitatively analyzed from the point of view of thermodynamics. For the transformation,

$$VO_2(A) \longrightarrow VO_2(R) \quad (1)$$

the thermodynamic criterion under conditions of constant temperature and pressure was the change of Gibbs free energy (ΔG), that is,

$$\Delta G = \Delta U + p\Delta V - T\Delta S \quad (2)$$

where U is the internal energy, p is the system pressure, V is the molar volume, T is the system temperature and S is the entropy. A process can occur only in the direction of decreasing Gibbs free energy, which means a spontaneous process leads to the minimum possible value of ΔG, and the sign for ΔG must be negative.

ΔG includes three items. Among them, for solid state materials, the effect of pressure on ΔU and ΔS is negligible when the system pressure is not extremely high, which was the case in our experiments (< 10 MPa). Since the phase transition from low-temperature VO_2(A) to high-temperature VO_2(A) occurs at 163 °C and the first-order phase transition from VO_2(M) to VO_2(R) takes place at 68 °C, in our hydrothermal treatment processes only three VO_2 polymorphs (VO_2(B), VO_2(A)(HT) and VO_2(R)) were involved at 270 °C. As reference, the ground state energies of VO_2(B), VO_2(A)(HT) and VO_2(R) were calculated by DFT using CASTEP code and they are shown in Fig. 4. Taking the energy of low-temperature metastable VO_2(B) phase as reference, the gap of ground state energies between high-temperature stable VO_2(R) phase and metastable VO_2(B) phase was 29.038 kJ/mol, while the corresponding energy gap between metastable VO_2(B) and VO_2(A)(HT) phases was 25.68 kJ/mol. The small energy gap between VO_2(A)(HT) and VO_2(R) destined the special metastable properties of VO_2(A). The data in Fig. 4 indicated that ΔU is negative with a relatively small absolute value in these three items in Eq. (2) corresponding to reaction 1. So the item of ΔU is not an overwhelming factor and it could not decisively determine the transformation direction of VO_2(A). For reaction 1, the item of $-T\Delta S$ is positive and is the obstacle for the transformation from VO_2(A) to VO_2(R). Based on the previous analysis, in this case the item of $p\Delta V$ should be regarded as a critical factor, which decisively determines that reaction 1 occurs spontaneously or that not. Table 2 lists the corresponding densities of VO_2 polymorphs. It was clear that the value of ΔV is negative, so the item of $p\Delta V$ is the only impetus in Eq. (2) for reaction 1 and higher pressure (p) should favor this transformation.

In order to confirm the hypothesis that the phase transformation can occur spontaneously under higher pressure, pre-synthesized VO_2(B) was placed in an autoclave as starting material under different filling ratios in the medium of deionized water and hydrothermally treated at 270 °C for 6 h. XRD patterns in Fig. 5

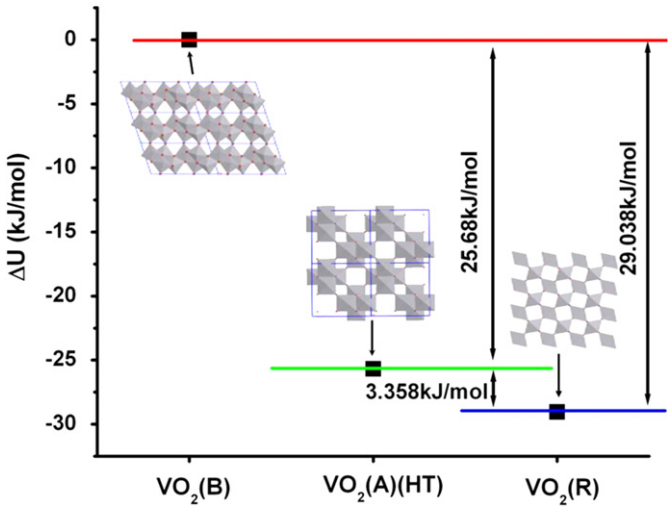

Fig. 4. The ground state energies of VO_2(B), VO_2(A) and VO_2(R).

Table 2
Densities of VO_2 polymorphs.

VO_2 polymorph	Density (g/cm^3)
VO_2(B)	4.031
VO_2(A)	4.035
VO_2(R)	4.67

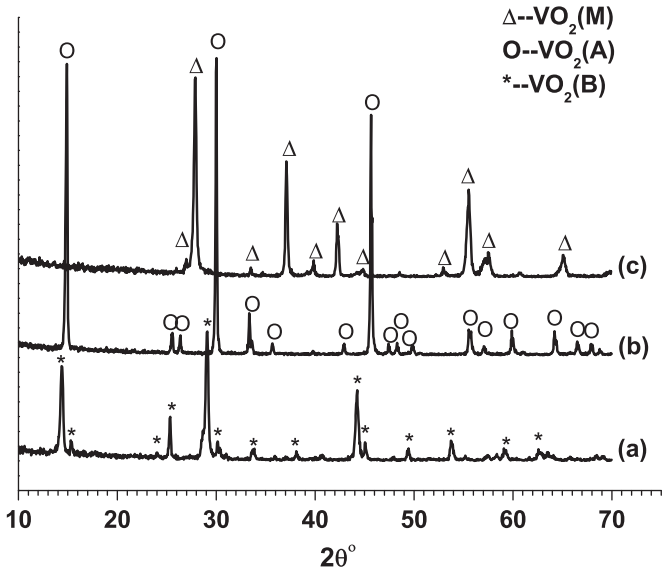

Fig. 5. XRD patterns for samples showing the pressure controlled phase transition for VO_2 polymorphs: (a) 180 °C/48 h; (b) 270 °C/6 h (f=0.60); (c) 270 °C/6 h ($f \approx 0.75$).

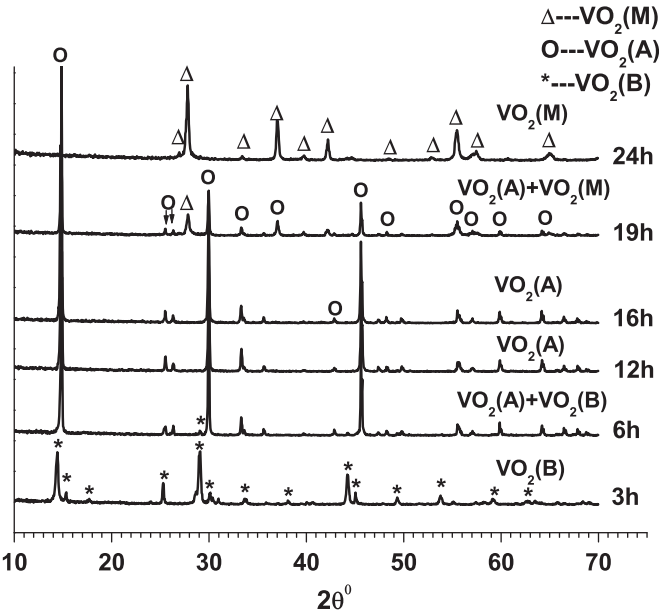

Fig. 6. XRD patterns for samples synthesized at 270 °C for different holding periods with the filling ratio of 0.50 (f=0.50).

showed the results of these verifiable experiments. When the filling ratio was 0.60, only VO_2(A) was resulted. By further increasing the filling ratio to about 0.75, the transformation from VO_2(B) to VO_2(R) was realized in our experiments. In the previous part, it has been disclosed that the auto-generated pressure was almost the same when the filling ratio was lower than 0.60 for water during hydrothermal treatment. This temperature-dependent pressure is even lower than the pressure for real solution under the filling ratio of 0.40 at 270 °C. So carefully increasing the filling ratio was the only method to elevate the auto-generated pressure. These results also indicated that the phase transition from VO_2(B) to other VO_2 polymorphs could be selectively controlled by system pressure.

The crystal structure dependent ground state energies in VO_2 system could also elucidate some other researchers' results reasonably. For example, even though extensive research for VO_2 has been carried out by many scientists in recent years, reports about the successful synthesis of pure VO_2(A) phase was very seldom. For another instance, there were some literatures that reported the results of annealing VO_2 hydrate or VO_2(B) for the formation of VO_2(R); however, the existence of VO_2(A) had usually not been observed during these processes. Due to the small energy gap between VO_2(A) and VO_2(R), the VO_2(B) or VO_2 hydrate would directly be transferred to stable VO_2(R) without careful control of annealing condition.

3.4. Crystallographic characteristics and transformation mechanisms for VO_2 polymorphs

To understand the mechanisms of the transformation from VO_2(B) to VO_2(A) and VO_2(A) to VO_2(R), serial experiments were carried out at 270 °C for different holding periods during hydrothermal treatment under the filling ratio of 0.50. XRD patterns for these samples in Fig. 6 clearly presented the phase evolution during hydrothermal treatment and the corresponding SEM images are shown in Fig. 7. In our system, VO_2(B) was always first formed and other polymorphs were derivatives from VO_2(B) with the extension of hydrothermal treatment time. It was found that in our experiments the yield was dependent on the holding time, filling ratio and temperature. When the reaction temperature was higher than 180 °C, more than 98% of the theoretical quantity of precipitation could be obtained after 24 h and the filtrate was very clear and colorless. The precipitate was formed gradually from the solution during hydrothermal treatment and higher auto-generated pressure resulting from higher filling ratio could accelerate this process. When the hydrothermal treatment was carried out under the filling ratio of 0.50, the basic reaction for the formation of VO_2 was over after 12 h (more than 98% of the theoretical quantity of precipitation could be collected and the phase transition from VO_2(B) to VO_2(A) happened in this period). Following the basic reaction it was the phase transformation from VO_2(A) to VO_2(R), which could happen spontaneously under higher pressure.

Since the steps for the formation of VO_2(A) from VO_2(B) and the transformation from VO_2(A) to VO_2(R) could be clearly distinguished in our experiments, the morphologies of these three phases could be easily confirmed from the SEM images. SEM images in Fig. 7 show that the crystal morphologies were very different between VO_2(B), VO_2(A) and VO_2(R). Analyzing the SEM images in Fig. 7 and combining the XRD results could draw the conclusion that VO_2(A) appeared as rod-like powders with a rectangle section (Fig. 7(d)) and the snowflake-like particles were the stable VO_2(R) phase (Fig. 7(f)). As shown in Fig. 7(a), VO_2(B) appeared as belt-like particles. SEM images in Fig. 7 also show that metastable VO_2(B) and VO_2(A) phases were preferentially grown along some particular crystal directions. The XRD patterns showed that (00n) serial peaks in VO_2(B) (see Fig. 2) were especially strong compared with the corresponding standard pattern in PDF card. The VO_2(B) nanobelt and VO_2(A) were also characterized by TEM. TEM image in Fig. 8(a) for the sample synthesized at 180 °C for 24 h showed that a typical VO_2(B) nanobelt was several micrometers in length, 30–100 nm in width and several to tens of nanometers in thickness. The selected area electron diffraction (SAED) pattern of an individual VO_2(B) nanobelt was inset in Fig. 8(a). This pattern was kept unchanged for different detected spots in one nanobelt, which means that VO_2(B) nanobelt was single crystal. The [010] direction in the electron diffraction pattern was parallel to the belt axis, showing that the growth of VO_2(B) nanobelts occurred along [010] direction, which was in agreement with the conclusion drawn from the XRD pattern.

While the single crystal VO_2(B) could be grown from the solution, single crystal rod-like VO_2(A) could not be obtained in

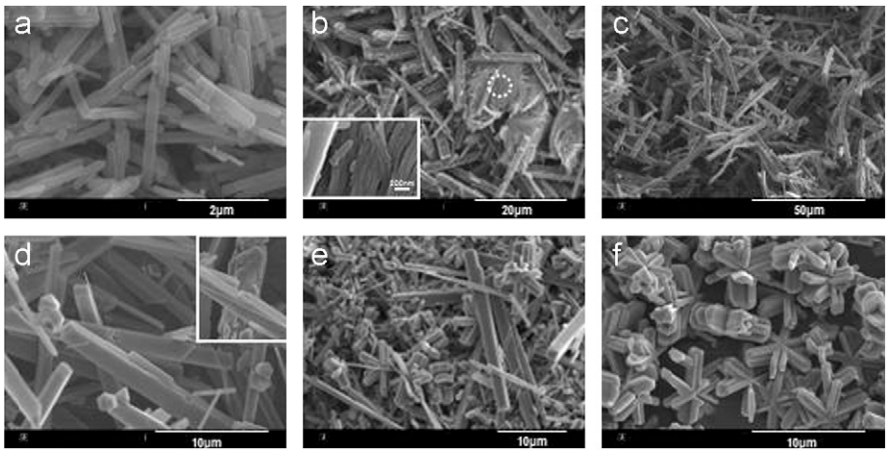

Fig. 7. SEM images for samples synthesized at 270 °C with the filling ratio of 0.50 (f=0.50) for different holding times: (a) 3 h, (b) 6 h, (c) 12 h, (d) 16 h, (e) 19 h, (f) 24 h. (Inset of (b) showed high magnification SEM image of the mixture of fibrous VO_2(B) and rod-like VO_2(A). Inset of (d) presented the transformation from VO_2(A) to VO_2(R) initialized from the volume shrinkage due to the formation of denser VO_2(R) embryo.)

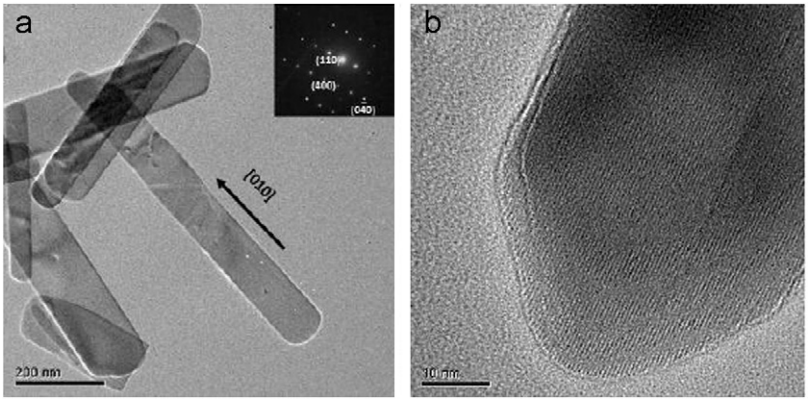

Fig. 8. TEM images for VO_2(B) (synthesized at 180 °C for 24 h) and VO_2(A) (synthesized at 230 °C for 24 h showing the formation of VO_2(A) from VO_2(B) by assembling).

our experiments. The formation of VO_2(A) should be started from the assembling of VO_2(B) nanobelts and then followed by a crystal structure adjustment. The trace of the assembling process could be clearly found in Fig. 8(b), which was a high resolution TEM image for the tip part of one VO_2(A) powder. Until now, direct synthesis of VO_2(A) could only be achieved via hydrothermal method. For the transformation of VO_2(A) from VO_2(B), Oka et al. [39] and Galy [40] proposed their mechanisms from a crystallographic view. Oka's proposal was based on the shift of oxygen vacancies along (010) planes in the f.c.c. VO_2(B) lattice with a rearrangement of vanadium atoms. Galy proposed a crystallographic slip, $C_s = 1/3[-100](001)$, in the mother VO_2(B) crystal network due to the weakest V–O bonding perpendicular to their medium plane (parallel to (001)). Their proposals were reasonable because there were some similarities between VO_2(B) and VO_2(A) from the point of crystallographic view. On one hand, they are constructed by the corner and edge sharing of vanadium–oxygen octahedra and the fourfold axes of the oxygen octahedra were aligned along one direction in VO_2(B) ([010]) and VO_2(A) ([001]), which was very different from the case of VO_2(R) in which its fourfold axes aligned along two perpendicular directions alternatively [26]. On the other hand, the densities (listed in Table 2) of VO_2(A) and VO_2(B) are very close. So the assembling of the VO_2(B) nanobelts could result in VO_2(A) by a simple crystallographic adjustment. While the phase transformation of VO_2(B) to VO_2(A) was considered as something like displacement-type one, the transformation of VO_2(A) to VO_2(R) was suitable to be treated as reconstructive change. Owing to the larger density difference between VO_2(A) and VO_2(R), there is a manifest volume shrinkage during the transformation from VO_2(A) to VO_2(R). SEM image of Fig. 7(d) indicated that the volume effect in this transformation led to the breakage of the rod-like VO_2(A) powder due to the formation of denser VO_2(R) embryos. During this process, the irregular polyhedra VO_2(R) embryos formed and then these embryos grew to snowflake-like VO_2(R) particles (Fig. 7(f)) through resolving and re-crystallization. The formation of the snowflake-like particles can be attributed to the static electricity attraction, which has been published in our previous works [41,42]. The mechanisms for the transformation of these VO_2 polymorphs were schematically depicted in Fig. 9.

3.5. Phase transition properties

Phase transition in VO_2 system has been studied widely especially for rutile-type VO_2(R) phase. The first-order metal-semiconductor phase transition (VO_2(R) to VO_2(M)) happens at 68 °C for single crystal. The principal feature of this transition is the formation and dissociation of V^{4+}–V^{4+} pairs. This feature was also observed in VO_2(B) phase over a temperature range from 300 to 180 K [43] and in VO_2(A) phase at 435 K [18] and it had been confirmed that a complete structural change could not be attained in these two VO_2 metastable polymorphs. DSC technology could be used to identify these phases because the thermal effect always accompanies the first-order phase transition. Fig. 10 shows some DSC curves tested from room temperature for typical samples. In these curves, the peaks appeared in lower temperature

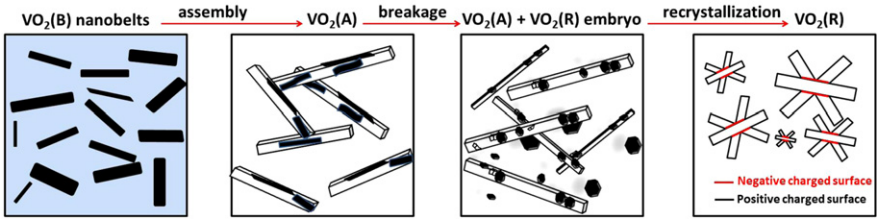

Fig. 9. Schematic chart shows the growing mechanisms from "VO_2(B)⟶VO_2(A)⟶VO_2(R)".

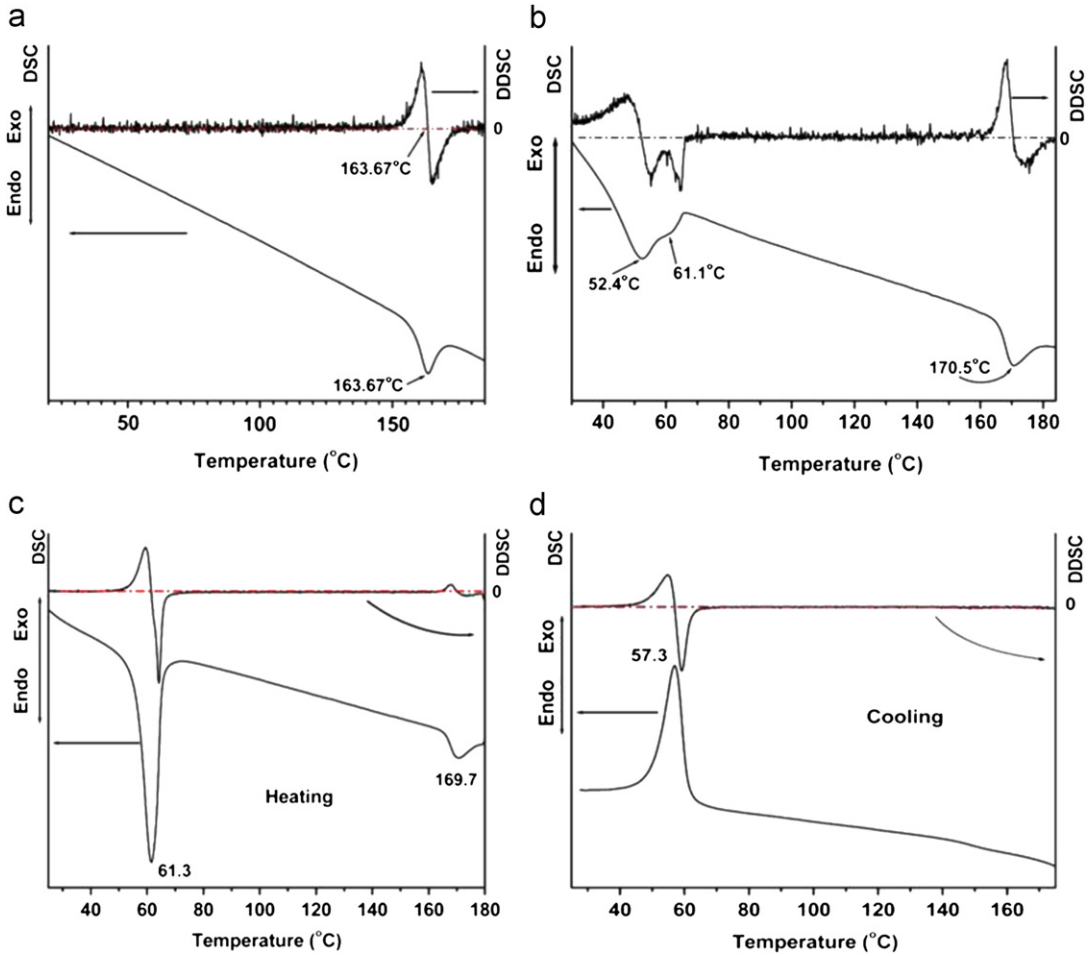

Fig. 10. DSC curves for samples synthesized at different conditions: (a) 270 °C /24 h, f=0.40, (b) 270 °C/16 h, f=0.50, (c,d) 270 °C/19 h, f=0.50 (recorded the heating and cooling processes separately).

side could be attributed to the phase transition between VO_2(R) and VO_2(M), while the peaks located at higher temperature side should be attributed to the phase transition between VO_2(A) polymorphs. Here DDSC was proposed for the determination of the phase transition temperature in DSC curves, that is,

$$\mathrm{DDSC} = \mathrm{dDSC}/\mathrm{d}T$$

where T is the temperature. DDSC is the differentiation of DSC, the point(s) of DDSC=0 corresponding to the extreme value(s) in DSC curve. Some interesting conclusions could be drawn through analyzing these curves.

Firstly, the phase transition temperatures for VO_2(A) could be modified by hydrothermal pressure under which those samples were synthesized. Oka et al. measured phase transition temperature of VO_2(A), which was 162 °C by DTA and magnetic susceptibility measurement and similar data have also been confirmed by us [30]. No other data about the phase transition temperature of VO_2(A) were available until now. In our experiments, the phase transition temperature during heating process for VO_2(A) prepared at relatively lower pressure (f=0.40) was similar with Oka's data. However, compared with those synthesized under relatively lower pressure (f=0.40, Fig. 10(a)), the phase transition temperature for VO_2(A) phase raised about 7 °C for samples synthesized under higher pressure (f=0.50, Fig. 10(b)). Secondly, DSC technology was an effective method to determine the presence of VO_2(R/M) and VO_2(A) phase and the thermal effects accompanied with the phase transition of VO_2(R) and VO_2(A) were distinctively different. Even though no peaks belonging to VO_2(R) could be indexed from the XRD pattern in Fig. 6 for sample synthesized at 270 °C holding for 16 h (f=0.50), two peaks contributing to VO_2(R) phase could be asserted from DSC curve in Fig. 10(b). It was consistent with the fact that some irregular polyhedra VO_2(R) embryos could be found in

Fig. 7(d). Fig. 10 also indicated that the thermal effect accompanied with the phase transition from VO_2(M) to VO_2(R) is stronger than those for VO_2(A). Studies indicated that the phase transition temperature of VO_2(R) depended on its crystal size, crystallinity and chemical constitution. Lower phase transition temperature for VO_2(R) during heating process and the broadening of the peaks in DSC curve might have resulted from lower crystallinity or nonstoichiometry of VO_2(R). With the increase in hydrothermal treatment time, the peaks in Fig. 10(c) and (d) belonging to VO_2(R) became sharp and the hysteresis gap became narrow.

4. Conclusions

Selective formation of VO_2(A) or VO_2(R) could be achieved by controlling the system pressure through varying the filling ratio during hydrothermal treatment. Calculation for the ground state energies of VO_2 polymorphs indicated that the energy gap between VO_2(A) and VO_2(R) is relatively small. By analyzing the change in the Gibbs free energy for the transformation from VO_2(A) to VO_2(R), the system pressure p was considered to be a critical factor, which decisively determines the direction of this transformation. It also means that the phase transformation from VO_2(A) to VO_2(R) is pressure sensitive. The results not only provide an effective way to control the desired morph of VO_2 but also help to profoundly understand the basic properties of these polymorphs, especially for metastable VO_2(A). Based on our experiments, VO_2(B) nanobelts were always first formed and then it transformed to VO_2(A) by an assembling process at increased temperature or extended reaction time. Under further higher pressure, the VO_2(A) transformed spontaneously to VO_2(R) initialized from the volume shrinkage due to the formation of denser VO_2(R). DSC measurement revealed that the phase transition temperature for VO_2(A) raised about 7 °C for samples synthesized under higher pressure and the thermal effects accompanied with the phase transition for VO_2(R/M) and VO_2(A) (HT/LT) were distinctively different.

Acknowledgments

The authors are grateful to K. Tajiri, M. Okada and M. Tazawa (AIST, Chubu, Japan) for valuable discussions and help for pressure measurements.

References

[1] S. Westman, Acta Chem. Scand. 15 (1961) 217.
[2] G. Andersson, Acta Chem. Scand. 10 (1956) 623.
[3] F. Theobald, R. Cabala, J. Bernard, J. Solid State Chem. 17 (4) (1976) 431.
[4] F. Theobald, J. Less Common Met. 53 (1) (1977) 55.
[5] D. Hagrman, J. Zubieta, C.J. Warren, L.M. Meyer, M.M.J. Treacy, R.C. Haushalter, J. Solid State Chem. 138 (1) (1998) 178.
[6] J. Galy, G. Miehe, Solid State Sci. 1 (6) (1999) 433.
[7] F.J. Morin, Phys. Rev. Lett. 3 (1) (1959) 34.
[8] A. Zylbersztejn, N.F. Mott, Phys. Rev. B 11 (11) (1975) 4383.
[9] J. Magarino, J. Tuchendler, J.P. D'Haenens, Phys. Rev. B 14 (3) (1976) 865–871.
[10] E. Strelcov, Y. Lilach, A. Kolmakov, Nano Lett. 9 (6) (2009) 2322.
[11] G. Guzman, F. Beteille, R. Morineau, J. Livage, J. Mater. Chem. 6 (3) (1996) 505.
[12] A.S. Oleinik, Tech. Phys. 47 (2002) 1014.
[13] C.G. Granqvist, Sol. Energy Mater. Sol. Cells 91 (17) (2007) 1529.
[14] G. Sudant, E. Baudrin, B. Dunn, J.-M. Tarascon, J. Electrochem. Soc. 151 (5) (2004) A666.
[15] E. Baudrin, G. Sudant, D. Larcher, B. Dunn, J.-M. Tarascon, Chem. Mater. 18 (18) (2006) 4369.
[16] H. Liu, Y. Wang, K. Wang, E. Hosono, H. Zhou, J. Mater. Chem. 19 (18) (2009) 2835.
[17] T. Yao, Y. Oka, N. Yamamoto, J. Solid State Chem. 112 (1) (1994) 196.
[18] Y. Oka, S. Sato, T. Yao, N. Yamamoto, J. Solid State Chem. 141 (2) (1998) 594.
[19] J.C. Valmalette, J.R. Gavarri, Mater. Sci. Eng. B 54 (3) (1998) 168.
[20] S. Chen, J. Lai, J. Dai, H. Ma, H. Wang, X. Yi, Opt. Express 17 (26) (2009) 24153.
[21] C. Tsang, A. Manthiram, J. Electrochem. Soc. 144 (2) (1997) 520.
[22] C. Zheng, X. Zhang, J. Zhang, K. Liao, J. Solid State Chem. 156 (2) (2001) 274.
[23] J. Liu, Q. Li, T. Wang, D. Yu, Y. Li, Angew. Chem. Int. Ed. 43 (38) (2004) 5048.
[24] G. Li, K. Chao, H. Peng, K. Chen, Z. Zhang, Inorg. Chem. 46 (14) (2007) 5787.
[25] X. Chen, X. Wang, Z. Wang, J. Wan, J. Liu, Y. Qian, Nanotechnology 15 (2004) 1685.
[26] C. Leroux, G. Nihoul, G. Van Tendeloo, Phys. Rev. B 57 (9) (1998) 5111.
[27] Z. Gui, R. Fan, W. Mo, X. Chen, L. Yang, S. Zhang, Y. Hu, Z. Wang, W. Fan, Chem. Mater. 14 (12) (2002) 5053.
[28] S.A. Corr, M. Grossman, Y. Shi, K.R. Heier, G.D. Stucky, R. Seshadri, J. Mater. Chem. 19 (25) (2009) 4362.
[29] Z. Gui, R. Fan, X.H. Chen, Y.C. Wu, J. Solid State Chem. 157 (2) (2001) 250.
[30] S. Ji, Y. Zhao, F. Zhang, P. Jin, J. Ceram. Soc. Jpn. 118 (1382) (2010) 867.
[31] W. Kohn, L.J. Sham, Phys. Rev. 140 (4A) (1965) A1133.
[32] R.O. Jones, O. Gunnarsson, Rev. Mod. Phys. 61 (3) (1989) 689.
[33] D.M. Ceperley, B.J. Alder, Phys. Rev. Lett. 45 (7) (1980) 566.
[34] J.P. Perdew, A. Zunger, Phys. Rev. B 23 (10) (1981) 5048.
[35] B.G. Pfrommer, M. Cote, S.G. Louie, M.L. Cohen, J. Comput. Phys. 131 (1) (1997) 233.
[36] Hydrothermal Science Handbook Editorial Committee, Handbook of Hydrothermal Science, Gihodo Press, Japan, 1997.
[37] G. Silversmit, D. Depla, H. Poelman, G.B. Marin, R. De Gryse, J. Electron Spectrosc. Relat. Phenom. 135 (2–3) (2004) 167.
[38] C.D. Wanger, G.E. Muilenberg, Handbook of X-ray Photoelectron Spectroscopy, Perkin-Elmer Corporation, 1979.
[39] Y. Oka, T. Yao, N. Yamamoto, J. Mater. Chem. 1 (5) (1991) 815.
[40] J. Galy, J. Solid State Chem. 148 (2) (1999) 224.
[41] S. Ji, F. Zhang, P. Jin, Mater. Lett. 65 (4) (2011) 708.
[42] S. Ji, Y. Zhao, F. Zhang, P. Jin, J. Cryst. Growth 312 (2) (2010) 282.
[43] Y. Oka, T. Yao, N. Yamamoto, Y. Ueda, A. Hayashi, J. Solid State Chem. 105 (1) (1993) 271.